Chem Soc Rev

REVIEW ARTICLE

The role of isovalency in the reactions of the cyano (CN), boron monoxide (BO), silicon nitride (SiN), and ethynyl (C_2H) radicals with unsaturated hydrocarbons acetylene (C_2H_2) and ethylene (C_2H_4)

Cite this: DOI: 10.1039/c3cs60328h

D. S. N. Parker,[a] R. I. Kaiser*[a] and A. M. Mebel*[b]

Received 16th September 2013

DOI: 10.1039/c3cs60328h

www.rsc.org/csr

The classification of chemical reactions based on shared characteristics is at the heart of the chemical sciences, and is well exemplified by Langmuir's concept of *isovalency*, in which 'two molecular entities with the same number of valence electrons have similar chemistries'. Within this account we further investigate the ramifications of the *isovalency* of four radicals with the same $X^2\Sigma^+$ electronic structure – cyano (CN), boron monoxide (BO), silicon nitride (SiN), and ethynyl (C_2H), and their reactions with simple prototype hydrocarbons acetylene (C_2H_2) and ethylene (C_2H_4). The fact that these four reactants own the same $X^2\Sigma^+$ electronic ground state should dictate the outcome of their reactions with prototypical hydrocarbons holding a carbon–carbon triple and double bond. However, we find that other factors come into play, namely, atomic radii, bonding orbital overlaps, and preferential location of the radical site. These doublet radical reactions with simple hydrocarbons play significant roles in extreme environments such as the interstellar medium and planetary atmospheres (CN, SiN and C_2H), and combustion flames (C_2H, BO).

[a] *Department of Chemistry, University of Hawai'i at Manoa, Honolulu, HI 96822, USA. E-mail: ralfk@hawaii.edu*

[b] *Department of Chemistry and Biochemistry, Florida International University, Miami, FL 33199, USA. E-mail: mebela@fiu.edu*

1. Introduction

In 1919 Langmuir coined the concept of *isovalency*, in which molecular entities with the same number of valence electrons

D. S. N. Parker

Dorian S. N. Parker received his PhD in Chemistry from University College London (United Kingdom) in 2009. He conducted postdoctoral work at the University of Hawaii, Chemistry Department using crossed molecular beams to investigate gas phase reaction dynamics in combustion and astrochemical environments. In 2013 he was awarded a postdoctoral fellowship with the NASA Astrobiology Institute (NAI) to study the role of neutral–neutral reactions in forming prebiotic molecules in extraterrestrial environments. His interests lie in the chemistry of extreme environments such as in combustion and astrochemistry, including the formation prebiotic molecules, as well as developing time-resolved imaging of reaction dynamics.

R. I. Kaiser

Ralf I. Kaiser received his PhD in Chemistry from the University of Münster (Germany) in 1994 and conducted postdoctoral work at UC Berkeley (Department of Chemistry). During 1997–2000 he received a fellowship from the German Research Council (DFG) to perform his Habilitation at the Department of Physics (University of Chemnitz, Germany) and Institute of Atomic and Molecular Sciences (Academia Sinica, Taiwan). He joined the Department of Chemistry at the University of Hawaii at Manoa in 2002, where he is currently Professor of Chemistry and Director of the W.M. Keck Research Laboratory in Astrochemistry. He was elected Fellow of the Royal Astronomical Society (UK) (2005), of the Royal Society of Chemistry (UK) (2011), of the American Physical Society (2012), and of the Institute of Physics (UK) (2013).

Table 1 Comparison table between four isovalent radicals CN, BO, SiN and C_2H

Chemical name	Cyano	Boron monoxide	Silicon nitride	Ethynyl
Formula	CN	BO	SiN	C_2H
Lewis structure	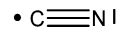	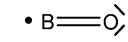	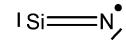	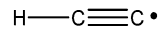
Bond energy (kJ mol^{-1})	749[44]	799[44]	438	728
I.E (eV)	13.6[45]	13.3 ± 0.5[45]	10.3[45]	11.61 ± 0.07[45]
E.A (eV)	3.862 ± 0.005	2.832 ± 0.008[45]	2.949 ± 0.001[46]	2.969 ± 0.001[45]
Internuclear distance (Å)	1.172	1.205	1.574	1.203
Bond order	Triple	Double	Double	Triple
Electronic structure	$X^2\Sigma^+$	$X^2\Sigma^+$	$X^2\Sigma^+$	$X^2\Sigma^+$

and the same electronic structure have similar chemistries.[1] The idea of isovalency allowed chemists to propel forward knowledge on reaction mechanisms involving organic and inorganic molecules based on their electronic structure. Small di- and tri-atomic radicals – cyano (CN; $X^2\Sigma^+$), boron monoxide (BO; $X^2\Sigma^+$), silicon nitride (SiN; $X^2\Sigma^+$), and ethynyl (C_2H; $X^2\Sigma^+$) have the same electronic structure and are *isovalent*. Gas phase collisionally induced reactions between these radicals and unsaturated hydrocarbons play significant roles in extreme environments such as extraterrestrial,[2,3] combustion,[4] and atmospheric environments[5] as well as in industrial settings like chemical vapor deposition (CVD).[6]

The majority of small reactive di- and tri-atomic species in the interstellar medium (ISM) are radicals, and their chemistry plays an important part in its chemical evolution.[5,7,8] The cyano (CN), silicon nitride (SiN), and ethynyl (C_2H) radicals have been identified in the ISM.[7,9–12] Cyanoacetylene (HCCCN) and vinyl cyanide (C_2H_3CN) were among the first nitriles molecules identified[13,14] and are thought to be formed through collisionally induced bimolecular reactions of the cyano radical with abundant acetylene and ethylene molecules, respectively.[15–20] A range of cyano radical reactions with unsaturated hydrocarbons can also explain the variety of cyano substituted molecules found in the hydrocarbon rich planetary atmospheres.[21–26]

A. M. Mebel

Alexander M. Mebel received his PhD in physical chemistry from Kurnakov's Institute of General and Inorganic Chemistry of Russian Academy of Science in Moscow, Russia. His first faculty appointment was at the Institute of Atomic and Molecular Sciences (Academia Sinica, Taiwan) and in 2003 he joined the Department of Chemistry and Biochemistry of Florida International University in Miami, Florida, USA, where he is currently Professor of Chemistry. His current research interests involve theoretical quantum chemical studies of mechanisms, kinetics, and dynamics of elementary chemical reactions related to combustion, atmospheric, and interstellar chemistry.

Reactions of ethynyl radicals with unsaturated hydrocarbons have also been proposed as a mass growth route to larger hydrocarbon molecules such as polycyclic aromatic hydrocarbons (PAHs) and polyacetylenes in the ISM and in planetary atmospheres.[22,27–33] The facile formation of PAHs by barrierless ethynyl additions is also important in combustion environments where formation of PAHs and eventually soot are unwanted competing reactions that negatively impact engine performance, health, and the environment.[27,34,35] The silicon nitride radical has also been identified in the interstellar medium such as in circumstellar envelopes of dying carbon stars[9] suggesting, based on the isovalency between cyano and silicon nitride, that the formation of organo-silicon molecules such as silaisocyanoacetylene and silaisocyanoethylene could follow similar mechanisms in extraterrestrial environments.[36–38] In CVD processes, silicon nitride reactions with unsaturated hydrocarbons are competing radical reactions that need to be correctly characterized in order to reduce their disruption.[6,39] Finally, in rocket propulsion systems the combustion of boron offers three times the energy release than carbon, however boron readily forms oxides like boron monoxide that disrupt the combustion process by undergoing competing reactions with fuel components such as unsaturated hydrocarbons.[40–43] The multitude of simultaneous reactions in extreme environments makes for a difficult area of study. Only by systematically investigating the chemical dynamics of each contributing elementary reaction under single collision conditions will we be able to effectively model these complex environments.

Table 1 summarizes the properties of the isovalent radicals CN, BO, SiN, and C_2H. The locations of the electron density corresponding to the radical can be understood in terms of each radicals Lewis structure. In cyano radical and boron monoxide the electron density of the radical preferentially resides on the most electropositive atom – carbon (2.55) and boron (2.04), compared with nitrogen (3.04) and oxygen (3.44), respectively. In cyano, carbon is left without its valency of 4 filled after forming a triple bond with nitrogen and nitrogen forms a lone pair, in boron monoxide, boron forms a double bond with oxygen leaving oxygen to form two lone pairs. Silicon nitride and the ethynyl radicals however, host their electron density on the more electronegative atoms: nitrogen (3.04) rather than the silicon atom (1.90), and carbon (2.55) rather than carbon bound to hydrogen (2.48). Here, silicon nitride only forms a double bond with nitrogen, presumably due to its large atomic radius, resulting in a lone pair residing on the

silicon atom and one lone pair on the nitrogen atom, and leaving the radical electron density to reside on the nitrogen atom. Similarly, carbons triple bond to C–H leaves one of its valences unfilled resulting in the electron density residing there. Despite the same number of valence electrons on each atom in silicon nitride and the cyano radical, the large silicon radius (1.10 Å) and diffuse p-type orbitals result in a significantly longer internuclear distance of 1.574 Å. Silicon's characteristic predisposition to form low order bonds is exhibited by the double bond in silicon nitride. Carbon on the other hand has a smaller radius of 0.85 Å and internuclear distance in the cyano radical of 1.172 Å formed by a triple bond with a bond energy 311 kJ mol^{-1} *stronger* than in silicon nitride. The longer and therefore weaker bond in the silicon nitride radical is also reflected in a reduced ionization energy. The ethynyl radicals triple bond is 21 kJ mol^{-1} less stable than the carbon–nitrogen triple bond of the cyano radical. Although the ethynyl radical benefits from optimal bonding overlap between the carbon atoms of the same radius, its bond energy is reduced due to the additional carbon–hydrogen bond. Boron monoxide is similar to the cyano radical in bond strength, ionization energy, and internuclear distance. However, boron monoxide's low electron affinity of 2.8 compared to the cyano group's 3.9 is indicative of the two lone pairs on the oxygen atom.

Generally, these isovalent species are *expected* to undergo similar chemistries to form isovalent products. However differing atomic compositions and radical locations cause significant divergences from their predicted chemical character. Within this article we shall discuss the chemical reactivity of small isovalent radicals that possess the electronic structure $X^2\Sigma^+$ – CN, BO, SiN and C_2H – with simple unsaturated hydrocarbon reactants acetylene (C_2H_2) and ethylene (C_2H_4), and as prototype representatives of organic molecules carrying a carbon–carbon triple (alkynes) and double (alkenes) bond.

2. The crossed molecular beam approach

The crossed molecular beam technique provides the unique ability to observe reactions between two molecules in the single collision regime – that is without wall effects or third body collisions.[47] This is achieved by generating molecular beams of reactants in separate chambers and colliding them into each other in the main reaction chamber (Fig. 1). The radical (CN, BO, SiN and C_2H) were formed *in situ* by laser ablation of a solid rod of carbon, boron, and silicon and subsequent co-reaction of the ablated species with a reactant gas (nitrogen, carbon dioxide, nitrous oxide and hydrogen) which also acted as a seeding gas as well. A chopper wheel was used to select a well-defined velocity of the pulsed radical beam, which in turn

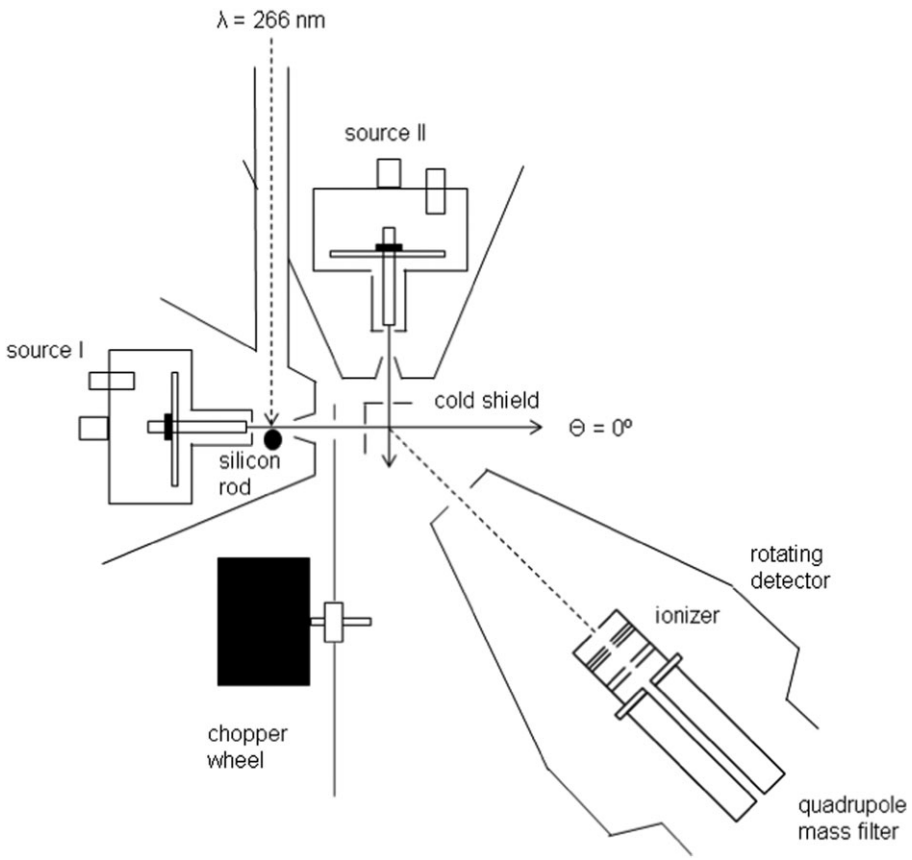

Fig. 1 Schematic top view of the crossed molecular beam apparatus. The two pulsed beam source chambers are defined as source I and source II, respectively. The silicon rod and the ablation laser source are incorporated in source I. The chopper wheel selects the appropriate primary beam velocity.

provides a specific kinetic energy of the primary beam reactant when undergoing reactive scattering with the secondary reactant, either acetylene or ethylene ($E_{collision}$ = 21–38 kJ mol^{-1}). The reaction products were monitored by a rotatable, triply differentially pumped mass spectroscopic detector within the plane of the primary and secondary beams. In this process, the neutral products are *universally* electron impact ionized at 80 eV before being mass selected at a specific mass-to-charge ratio (m/z) and detected under ultra high vacuum conditions (3×10^{-12} Torr). The reactive scattering signal at a specific mass-to-charge ratio is recorded at multiple angles exploiting the time-of-flight (TOF) technique. Here, the ion counts of an ion of the selected mass-to-charge ratio (m/z) are recorded *versus* the time. The collision between the radical and the hydrocarbon defines the 'time zero' in each experiment. At each angle, the TOFs are integrated furnishing us with the laboratory angular distribution, *i.e.* a distribution reporting the integrated ion counts at a defined mass-to-charge ratio *versus* the laboratory angle. These laboratory data (laboratory angular distribution, TOF spectra) are transformed into the center-of-mass reference frame *via* a forward deconvolution technique. This yields two crucial functions, which – together with the laboratory data – assist us to extract the reaction dynamics and underlying reaction mechanisms: the center-of-mass angular distribution ($T(\theta)$) and the product translational energy distribution ($P(E_T)$).

3. Electronic structure calculations

Obtaining accurate potential energy surfaces for each crossed beam reaction is an integral part of elucidating the reaction mechanisms and products formed. In this review we cover eight potential energy surfaces covering theoretical work spanning over a decade and therefore covering a range of theoretical methods. Here, we will describe the general approach in uncovering the chemical routes available in bimolecular collisions between CN, BO, SiN and C_2H with acetylene and ethylene, respectively. Firstly, structures of the reactants, products, intermediates, and transition states on their respective potential energy surfaces were optimized at the hybrid density functional B3LYP level[48,49] with the 6-311G** basis set and vibrational frequencies were calculated using the same B3LYP/6-311G** method. From here, higher level methods, such as the coupled cluster CCSD(T) method[50] with Dunning's correlation-consistent cc-pVTZ basis set[51] were used to refine relative energies of various structures. Any open shell structures were subsequently calculated with spin-restricted coupled cluster RCCSD(T). These calculations were carried out using program packages GAUSSIAN[52] and MOLPRO.[53] In specific cases further calculations were conducted using CCSD(T)/cc-pVDZ, CCSD(T)/cc-pVQZ, and CCSD(T)/cc-pV5Z to extrapolate their CCSD(T) total energies to the complete basis set (CBS) limit.[54] The equation $E_{tot}(x) = E_{tot}(\infty) + Be^{-Cx}$, was fitted where x is the cardinal number of the basis set (2, 3, 4, and 5 for cc-pVDZ, cc-pVTZ, cc-pVQZ, and cc-pV5Z, respectively) and $E_{tot}(\infty)$ is the CCSD(T)/CBS total energy. It is anticipated that by these theoretical methods relative energies are accurate within 5–10 kJ mol^{-1}.

4. Results and discussion

Here, we review the results of our crossed molecular beam experiments of four isovalent $X^2\Sigma^+$ radicals – CN,[15,17,28] BO,[40,41] SiN,[37,38] and C_2H[28,55,56] – with simple prototypical hydrocarbon reactants, acetylene (C_2H_2) and ethylene (C_2H_4). This approach will help us to elucidate generalized concepts on the chemical dynamics and the similarities and differences of the underlying mechanisms of the reactions of isovalent radicals with unsaturated hydrocarbons in extreme environments and their role in the formation of substituted hydrocarbons.

4.1 Reactive scattering

Reactive scattering signal was detected at mass-to-charge ratios (m/z) of 51 (CNC_2H^+),[15] 52 (BOC_2H^+),[40] 67 ($SiNC_2H^+$)[37] and 50 ($C_2HC_2H^+$)[17] for reactions with acetylene (Fig. 2a and c) and mass-to-charge ratios (m/z) of 53 ($CNC_2H_3^+$),[16] 54 ($BOC_2H_3^+$),[14] 69 ($SiNC_2H_3^+$)[12] and 52 ($C_2HC_2H_3^+$)[18] for reactions with ethylene (Fig. 2b and d). For all systems studied, ion counts were also detected at lower mass-to-charge ratios. However, the TOF spectra were found to be exactly superimposable to the higher mass-to-charge signals. Therefore, the lower mass-to-charge ratios can be associated with dissociative ionization of the product in the electron impact ionizer. The recorded signal at the mass-to-charge ratios correspond to a product formed between the radical and the hydrocarbon reagents *via* a radical *versus* hydrogen atom exchange mechanism. The molecular formulas of the products are shown above together with their distinct mass-to-charge ratios used to identify them in each experiment. In the reactions involving the CN, BO, and SiN radicals, the hydrogen can only originate from the hydrocarbon reactant acetylene or ethylene. With the ethynyl (C_2H) radical it was necessary to use deuterated reactants, such as D1-ethynyl (C_2D) or D2-acetylene (C_2D_2) to determine whether the hydrogen was emitted from the ethynyl (C_2H) radical or the hydrocarbon reactant. In the reaction of C_2D[17] with C_2H_2 and C_2H[18] with C_2D_2, data were collected at m/z = 51 [C_4HD] and m/z = 55 [C_4HD_3] indicating a light atom [D/H] was emitted from acetylene and ethylene, respectively. In summary, in reactions of isovalent $X^2\Sigma^+$ radicals – CN, BO, SiN, and C_2H with small hydrocarbons, a radical *versus* atomic hydrogen exchange reaction is undertaken, and the light atom emission is solely from the hydrocarbon reactant. It should be noted that the molecular formula as determined by the mass spectra signal is insufficient to determine the molecular structure of the product isomer formed.

To gain the necessary insight into the product isomer(s) formed, the laboratory data are converted into the center-of-mass frame, providing information on the energetics and reaction mechanism(s). Using a forward convolution routine, a translational energy distribution, $P(E_T)$, and center-of-mass angular distribution, $T(\theta)$, are generated for each cross beam

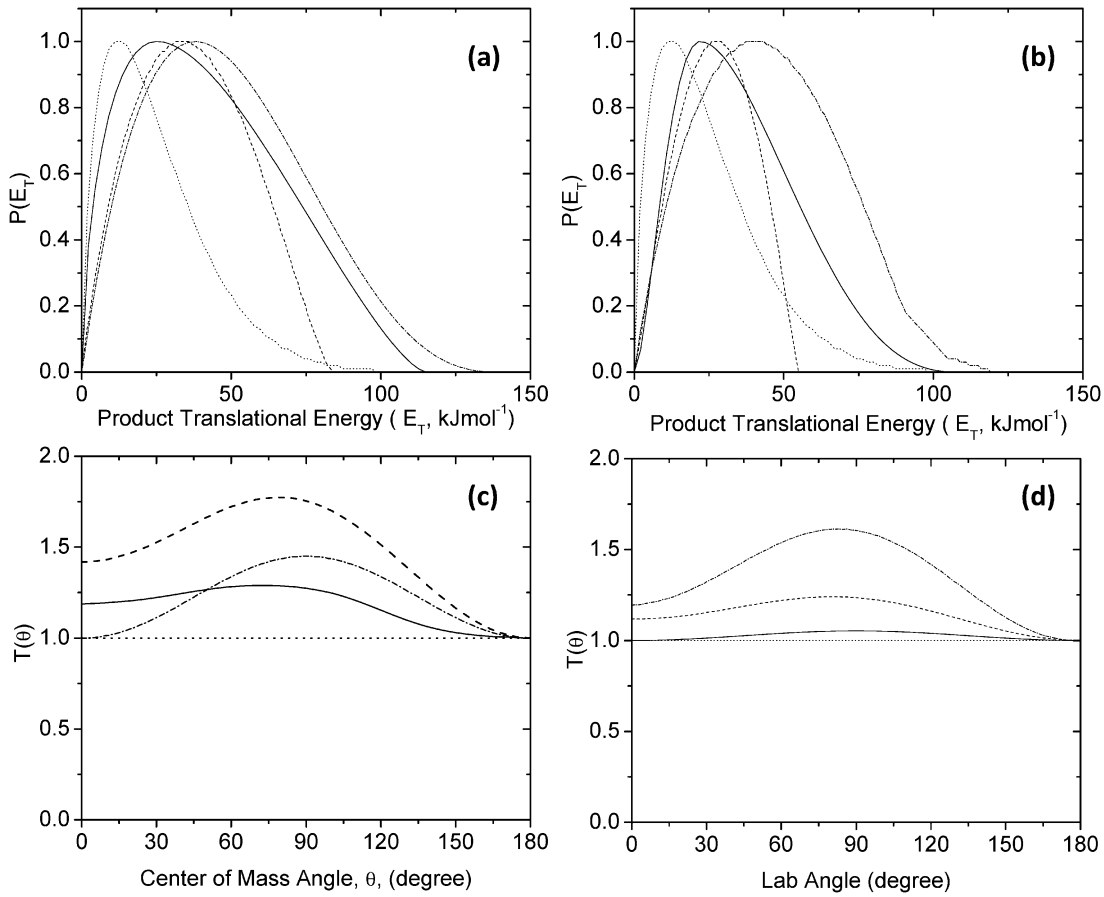

Fig. 2 Center of mass translational energy $P(E_T)$ (a and b), and center of mass angular distributions $T(\theta)$ (c and d) in the reactions of radicals with acetylene (a and c) and ethylene (b and d). Radical line designations: cyano (CN) solid, boron monoxide (BO) dashed, silicon nitride (SiN) dotted, ethynyl (C_2H) dot dashed.

reaction as shown in Fig. 2. The maximum translational energy of the $P(E_T)$ indicates the total energy of the reaction, which is composed of the collision energy plus the reaction energy, and is associated with the energy of breaking and reforming chemical bonds. The reaction energy can be used to identify the product formed in the reaction, either through comparison to reaction energies available in the literature or from values calculated using electronic structure calculations such as those shown in Fig. 3 and 4. The reaction energies of the heavy product formation through hydrogen atom emission for the radical reactions with acetylene were 90 ± 10 kJ mol^{-1} [HCCCN], 62 ± 8 kJ mol^{-1} [HCCBO], 54 ± 22 kJ mol^{-1} [HCCNSi] and 110 ± 10 kJ mol^{-1} [HCCCCH], and for reactions with ethylene 110 ± 10 kJ mol^{-1} [C_2H_3CN], 54 ± 13 kJ mol^{-1} [C_2H_3BO], 64 ± 24 kJ mol^{-1} [C_2H_3NSi], and 94 ± 20 kJ mol^{-1} [C_2H_3CCH]. In each case, the reaction energy was compared to theoretical calculations for distinct isomers (Fig. 3 and 4). For the reactions involving acetylene and the isovalent radicals CN, BO, SiN, and C_2H (Fig. 3a–d) depict an excellent agreement in the formation of cyanoacetylene (HCCCN; −78 kJ mol^{-1}), boronylacetylene (HCCBO; −58 kJ mol^{-1}), silaisocyanoacetylene (HCCNSi; −68 kJ mol^{-1}), and diacetylene (HCCCCH; −118 kJ mol^{-1}) together with atomic hydrogen. Similarly, the reactions involving ethylene show excellent correlation with the formation of atomic hydrogen and vinyl cyanide (C_2H_3CN; −95 kJ mol^{-1}), boronylethylene (C_2H_3BO; −39 kJ mol^{-1}), silaisocyanoethylene (C_2H_3NSi; −66 kJ mol^{-1}), and vinylacetylene (C_2H_3CCH; −110 kJ mol^{-1}). The translational energy distributions all depict a maximum away from zero translational energy; this finding is indicative of the existence of exit barriers and tight exit transition states, here, ranging from 7–30 kJ mol^{-1} above the separated products. These order-of-magnitudes agree well with the exit barriers depicted in Fig. 3 and 4, respectively. Considering the principle of microscopic reversibility, the reversed reactions of hydrogen addition to the closed shell products have entrance barriers of this order of magnitude.

The center-of-mass angular distributions, $T(\theta)$, derived from the fits to the experimental data also provide additional insights into the reaction dynamics. The center-of-mass angular distributions for all systems show intensity over the full angular range; this finding is indicative of indirect, complex-forming reaction mechanisms. This means the reactions involve the formation of collision complexes: C_2H_2CN, C_2H_2BO, C_2H_2NSi, and $C_2H_2C_2H$ for acetylene reactions and C_2H_4CN, C_2H_4BO, C_2H_4NSi, and $C_2H_4C_2H$ for the ethylene

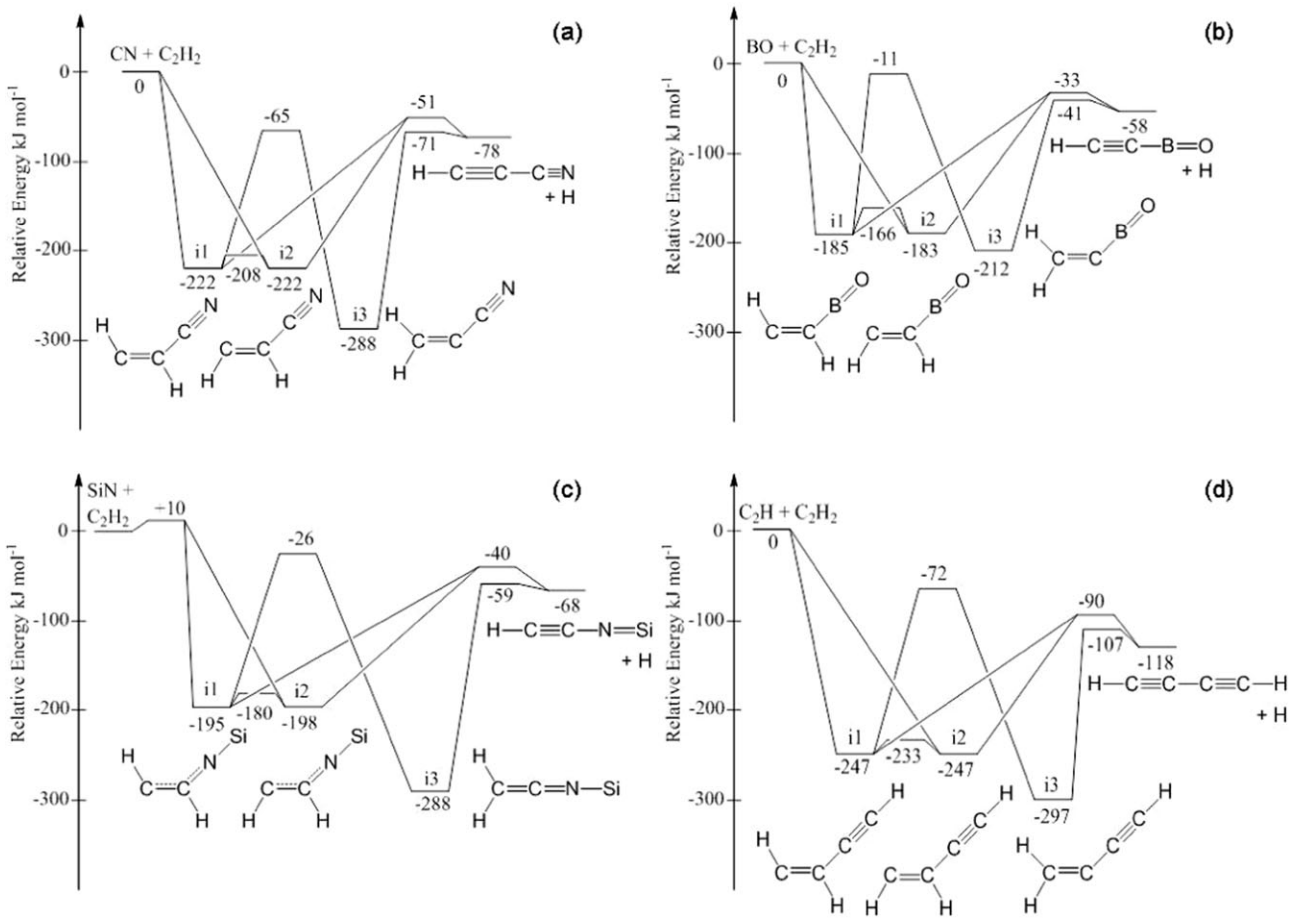

Fig. 3 Potential energy surfaces of the product forming reaction pathways in radical reactions with acetylene (a) cyano (CN) (b) boron monoxide (BO), (c) silicon nitride (SiN), (d) ethynyl (C_2H) radicals.

reactions. Since the reactions between the radical and hydrocarbon reactants are conducted in the gas phase under single collision conditions, all intermediates fragment as a result of the high internal energy accrued from the collision energy and the bond formation. Further, the $T(\theta)$s depict a higher flux in the direction of the radical beam indicating that the lifetimes of the complexes are comparable and/or shorter than the rotational period of the complex (osculating complex behavior).[57] The shape of the center-of-mass angular distribution is also dictated by the disposal of the total angular momentum, J. The reactants undergo rotational cooling in a supersonic expansion resulting in the initial total angular momentum, J, being equivalent to the orbital angular momentum L, and due to conservation of momentum, also equivalent to the final orbital angular momentum L', to give: $J \approx L \approx L'$. The final recoil velocity vector v', is perpendicular to L' and therefore in the plane perpendicular to J. The center-of-mass scattering angle θ, is defined as the angle between the initial relative velocity v and v', and depends on the values of J, M and M', where M and M' are the projections of J on the initial and final relative velocity, respectively. In a collision complex that dissociates with high M' values, the final relative velocity will be almost parallel to J and perpendicular to v and the products will be preferentially scattered at $\theta = 90^\circ$. Grice and Smith have used microcanonical theory to understand the reaction OH + CO → CO_2 + H, which passes through a bent, nearly-linear reaction intermediate, similar to the reaction intermediates formed in the present reactions.[58] The authors calculated and experimentally demonstrated that for a prolate linear rotor with an angle between the exiting hydrogen atom and the primary rotation axis, A, of $\beta = 90^\circ$ would produce a heavily peaked center-of-mass angular distribution. They also calculated that with $\beta = 45^\circ$, the angular distribution would be broad peaked. Each experiment presented fits into the same premises for Grice and Smith's model; the exiting species are light hydrogen atoms, each hydrogen emission has an exit barrier, and the intermediate can be considered as a linear rotor.

Now we shall discuss the reactions in further detail, each reaction depicts peaked, and often heavily peaked, center-of-mass angular distributions which are indicative of a preferential hydrogen loss direction perpendicular to the rotational plane of the decomposing complex on the reaction pathway taken to the product. Let us consider the structures of the intermediates prior to hydrogen loss that are able to form in the reaction: for acetylene reactions these are i1–i2 (*trans*-CHCHX–*cis*-CHCHX) intermediates or i3 CH_2CX, for ethylene reactions

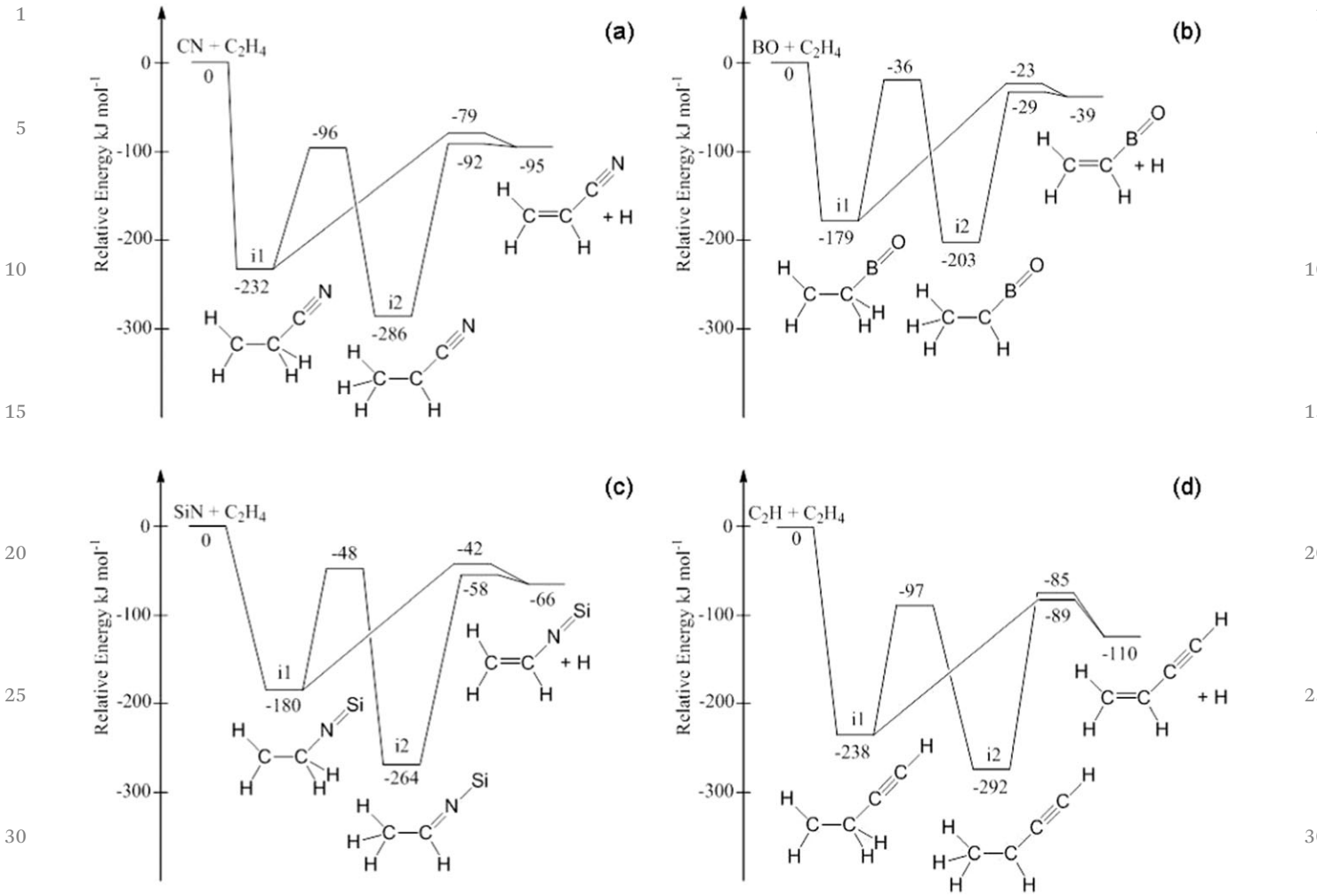

Fig. 4 Potential energy surfaces of the product forming reaction pathways in radical reactions with ethylene (a) cyano (CN) (b) boron monoxide (BO), (c) silicon nitride (SiN), (d) ethynyl (C_2H) radicals.

these are i1 CH_2CH_2X or i2 CH_3CHX. In both acetylene and ethylene reactions H atom loss can either occur from the primary carbon or from the secondary carbon. In acetylene reactions, emission from the primary carbon is constrained to be near 90° relative to the rotational plane of the near-linear intermediate i1–i2, an emission direction which causes strong peaking. The hydrogen emission from the secondary carbon is about 2–5° larger than from the primary carbon. This is due to the free rotation of either of the two hydrogen atoms around the secondary carbon in comparison to the single hydrogen on the near linear rigid carbon backbone of the primary carbon. The greater free rotation will blur the angle relative to the orbital angular momentum and therefore reduce the prominence of the peaking in the center-of-mass angular distribution. In these respects, the heavily peaked angular distributions shown in Fig. 2 indicate emission from i1 is the dominant route taken in the acetylene reactions, which is supported by RRKM theory that specifies only a few percent isomerize to i3 CH_2CX and the dominant reaction pathway is through hydrogen emission from i1–i2 (*trans*-CHCHX–*cis*-CHCHX) intermediates. In the ethylene reactions the distinctions between hydrogen emission from the primary and secondary carbons is further blurred by the existence of an extra hydrogen on each carbon. Here, the extra hydrogen on the primary carbon forces the molecule to be further bent, and along with another hydrogen atom, forces the emitting hydrogen angles to be spread over a greater range. Hydrogen emission from the CH_3 group on the secondary carbon is expected to be less perpendicular to the rotation plane than emission from the primary carbon. The less pronounced peaking of $T(\theta)$ in the ethylene reaction reflects the less perpendicular emission angles, although peaking is still present indicating some preferential emission direction. The RRKM theory branching ratios reflect these observations stating that about 50–70% tend to pass through the intermediate i2 CH_3CHX and the remainder 50–30% through intermediate i1 CH_2CH_2X. It should be noted that, the silicon nitride reactions are depicted as isotropic however, the error boundaries show a forward scattering and peaking are also able to adequately fit the data. In contrast the high signals from the boron monoxide experiments manifest as strong peaking and cannot be fit with isotropic distributions. Therefore, the degree of peaking between the different systems should not be over

interpreted due to the significantly differences in overall signal to noise levels between each experiment.

4.2 Potential energy surfaces

The exploitation of electronic structure calculations is an integral part of the present study to unravel the complex reaction dynamics of bimolecular reactions. Here, *ab initio* calculations provide the potential energy surfaces (PESs), which reveals possible reaction intermediates and products formed together with transition states interconnecting them. These data can be then compared with the experimental results. We find that the reactions are able to proceed through addition of the atom with the radical centred on it to the triple bond of acetylene and the double bond of ethylene to reach intermediate (i1–i2) shown in Fig. 3 and 4. Table 1 shows the structures of the radical, with the location of the atom which has the radical centred on it. For CN, BO, SiN, and C_2H the radical is centred on C, B, N and C respectively, and these are the atoms which bind to the carbon–carbon triple and double bonds of the hydrocarbon reactants. In the reactions of CN, BO, and C_2H the barrierless binding of the radical to acetylene may create both *trans*-CHCHX and *cis*-CHCHX intermediates. For the SiN reaction, the SiN addition transition state exhibits a *trans*-CHCHX conformation but the CCH fragment is nearly linear, so that both *trans* and *cis* conformers of the adduct can be created on the downward path after the entrance barrier is cleared. Considering the ethylene reactions, all radicals bind to ethylene to form a CH_2CH_2X intermediate (i1) (Fig. 4a–d). These additions for both the acetylene and ethylene systems proceed without an entrance barrier to the initial intermediate structure (i1) except for the reaction of silicon nitride with acetylene, which has a 10 kJ mol^{-1} entrance barrier. The barrierless nature of all other reactions implies that they could proceed in ultracold environments like in cold molecular clouds holding averaged temperatures of 10 K. In all reactions with acetylene the initial *trans*-CHCHX intermediate (i1) can undergo a *trans–cis* isomerization to the *cis*-CHCHX intermediate (i2) by overcoming a small barrier of 14–22 kJ mol^{-1}. From the *cis*-CHCHX intermediate (i2), a hydrogen emission from the C2 carbon leads to the product channels HCCX plus atomic hydrogen through a tight exit transition state of between 22–28 kJ mol^{-1}. In fact, the H loss transition states exhibit linear or nearly linear CCH fragments, indicating that the minimal energy path from these transition states backward may bifurcate and lead both to *cis* and *trans* intermediates (i2) and (i1). This means that both (i1) and (i2) can eliminate a hydrogen atom *via* the same transition state. An alternative route, for all the acetylene reactions, involves a hydrogen migration from the CHCHX structures reaching the CH_2CX type structure (i3), which represents the global minimum of 212–297 kJ mol^{-1} relative to the reactants. From the CH_2CX intermediates (i3), the product channel HCCX plus atomic hydrogen is reached through a tight exit transition state, associated with hydrogen emission from the terminal carbon atom C1. The reaction pathway through intermediate (i3) has an exit barrier around half that for the reaction pathway from the *trans*-CHCHX intermediate (i2). The CN, BO, SiN, and C_2H reactions with ethylene also have a pathway to the products CH_2CHX plus atomic hydrogen from the initial CH_2CH_2X intermediate (i1) *via* a hydrogen emission from the central C2 carbon, through tight exit transition states positioned between 16 and 24 kJ mol^{-1} above the final products. Alternatively, the initial intermediate (i1) can undergo a hydrogen migration from C2 to C1 to reach the global potential minimum structure CH_3CHX (i2). The CH_3CHX intermediate (i2) can subsequently emit a hydrogen atom from the CH_3 group to reach the products CH_2CHX plus hydrogen through a tight exit transition state lying between 3 and 25 kJ mol^{-1} above the products.

5. Structure and bonding character of product isomers

In this *Review*, we have reported information on the chemical dynamics, involved collision complexes, reaction intermediates, energetics, and products of the isovalent reactions of the $X^2\Sigma^+$ radicals CN, BO, SiN, and C_2H with small, prototype unsaturated hydrocarbon molecules acetylene (C_2H_2) and ethylene (C_2H_4). In all cases the reactions were found to undergo a radical *versus* hydrogen exchange; the primary products were identified as cyanoacetylene, boronylacetylene, silaisocyanoacetylene, and diacetylene [acetylene reactions] as well as vinyl cyanide, boronylethylene, silaisocyanoethylene, and vinylacetylene [ethylene reactions]. The reactions were all found to proceed through addition of the atom with the radical centred on it, *i.e.* C, B, N, and C in CN, BO, SiN and C_2H, respectively, to the π electron density of the reactant *via* indirect scattering dynamics. In acetylene and ethylene systems, HCCX and C_2H_3X products, respectively, could be reached through emission of a hydrogen atom either from the primary carbon or – after a hydrogen shift – from the secondary carbon. Both reaction channels are energetically comparable and result in product formation *via* tight exit transition states.

It is fascinating to compare the structure of the products formed in these isovalent reactions. The reaction products and their corresponding bond lengths are shown in Fig. 5 and 6.

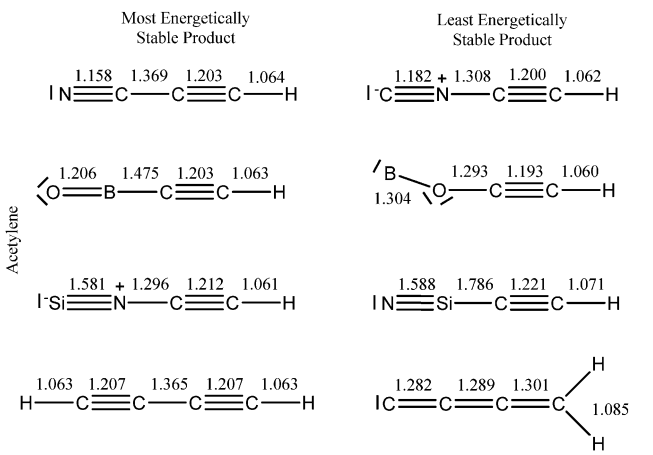

Fig. 5 Bond lengths in Angstroms (Å) of the reaction products formed *via* $X^2\Sigma^+$ radical reactions (CN, C_2H, BO and SiN) with acetylene.

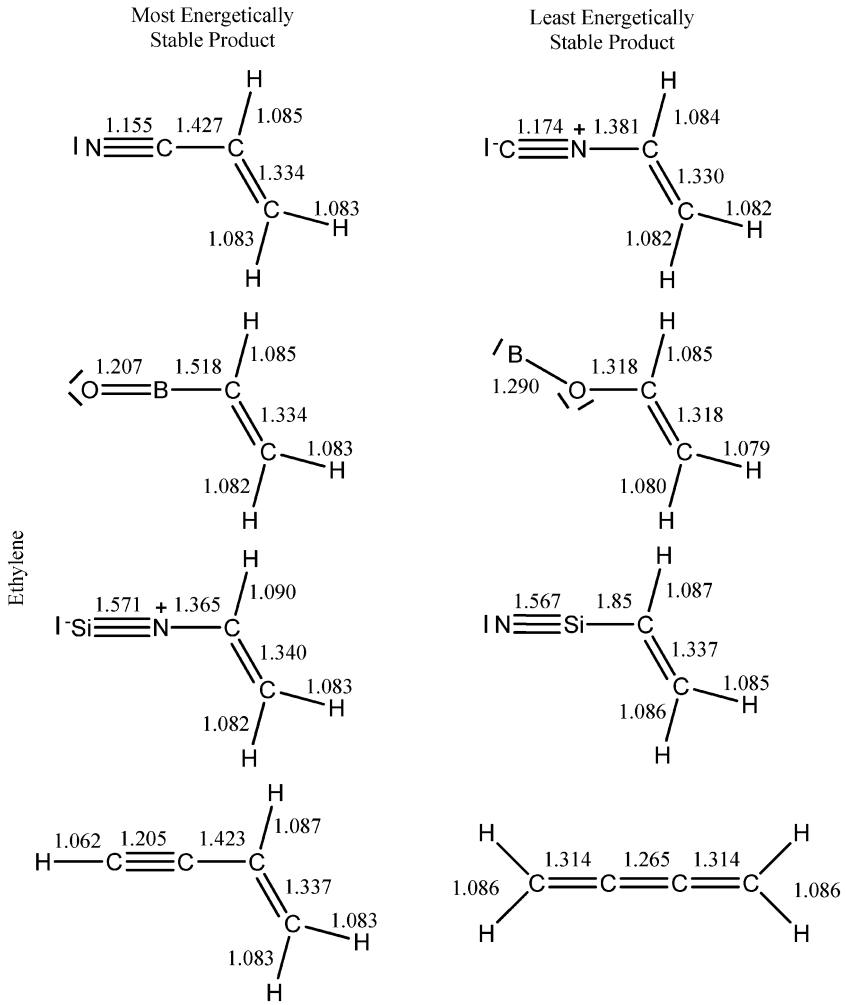

Fig. 6 Bond lengths in Angstroms (Å) of the reaction products formed *via* $X^2\Sigma^+$ radical reactions (CN, C_2H, BO and SiN) with ethylene.

Despite the clear relationship between radical location and product structure, the resulting product must be interpreted in terms of its structural characteristics, *i.e.* the stability of its relative product isomers and not necessarily on the initial intermediate formed. The initial intermediate is formed by bonding of the radical to the reactant producing a collision complex. Depending on the reaction pathways available, the collision complex is able to isomerize. To better understand the relative stability of the product isomers the bond lengths, Lewis structures, symmetries and static charges of the product isomers have been shown in Fig. 5 and 6 and are grouped into the most energetically stable structures on the left and next closest contender in terms of energetic stability named the least energetically stable isomer on the right. It should be noted that more than two product isomers exist in all cases but have been omitted due to relevance and clarity. The most energetically stable isomers are those products with the radical bearing atom bound to the secondary reactant and the least energetically stable isomer has the non radical bearing atom bound to the reactant, except in the case of ethynyl reactions.

The product isomer cyanoacetylene (HCCCN) has a bond length between the carbon of the cyano group and carbon of the ethynyl group of 1.369 Å; it has a stable Lewis structure with a lone pair on the nitrogen atom and no static charges. The isocyanoacetylene molecule (HCCNC) on the other hand has a shorter N–C bond length of 1.308 Å between the radical and the acetylene molecule; it has formal charges on the nitrogen and carbon atoms. The short bond length is due to the smaller atomic radius of nitrogen of 0.65 Å compared with that of carbon which is 0.70 Å. The nitrogen atom's bonding orbitals are smaller and require closer proximity to those of carbon to achieve efficient bonding overlap. In comparison, carbon–carbon bonding in cyanoacetylene benefits from ideal orbital overlap between the carbon atom of the radical and the carbon atom of the ethynyl group, each of the carbon atoms bonding orbitals are of the same size and shape and therefore offer the best bonding overlap. This is inline with the well known fact that carbon–carbon bonding is highly efficient, especially when conjugated. Here, the radical – hydrocarbon bond has the greatest impact on the stability of cyanoacetylene with the N–C bond being too short compared to the ideal carbon–carbon bond length in cyanoacetylene causing the isocyanoacetyene isomer to be 117 kJ mol^{-1} less stable. The shorter N–C bond

length in isocyanoacetyene (HCCNC) also adversely lengthens the carbon–nitrogen triple bond. The carbon–nitrogen bond of the cyano group is elongated to 1.182 Å compared to 1.158 Å of the nitrogen–carbon triple bond in cyanoacetylene. The change in the cyano group bond length is also representative of the change in formal charge of nitrogen and carbon of +1 and −1, respectively. The cyano plus ethylene product isomers show much the same characteristics as the acetylene product isomers, with the vinyl cyanide (C_2H_3CN) product isomer having a short N–C bond of 1.381 Å and long C–N triple bond of 1.174 Å, compared to that in vinyl isocyanide (C_2H_3NC) of 1.427 Å for the C–C bond and 1.155 Å for the N–C triple bond. In the unfavorable vinyl isocyanide molecule, there are static charges of +1 on the nitrogen and −1 on the carbon, while on the vinyl cyanide molecule, the electrons are perfectly balanced, highlighting their respective stabilities that differ by about 100 kJ mol^{-1}. The bond lengths in the rest of the molecule *i.e.* the carbon–hydrogen and carbon–carbon double bond show a marginal change and so have little influence over the energetic stability of the molecule.

In considering the boron monoxide (BO) reactions, the radical bonds preferentially with its boron atom to the hydrocarbon reactant rather than with the oxygen atom. Boron's atomic radius (0.85 Å) is closer to that of carbon's (0.70 Å) than to oxygen (0.60 Å) resulting in better bonding overlap with the hydrocarbon reactant. The enhanced bonding between the orbitals of boron and the π-system results in a stronger bond, making boronylacetylene (HCCBO) and boronylethylene (C_2H_3BO) more stable than isoboronylacetylene (HCCOB) and isoboronylethylene (C_2H_3OB), respectively. In the energetically favorable boronylacetylene (HCCBO) and boronylethylene (C_2H_3BO) molecules, the valence electrons of boron are fully utilized in bonding orbitals, and the oxygen has its two lone pairs located away from the rest of the molecule. The tight bonding of oxygen and boron in boronylacetylene (HCCBO) and boronylethylene (C_2H_3BO) results in bond lengths of 1.206 Å and 1.207 Å indicative of double bonds and giving B–C bond lengths of 1.475 Å and 1.518 Å. Conversely, in the unfavorable geometries the B–O bond is 1.304 Å and 1.290 Å for isoboronylacetylene (HCCOB) and isoboronylethylene (C_2H_3OB), respectively representing single bonds. The O–C bond lengths in these molecules are 1.293 Å and 1.318 Å representing standard single bond distances.

In the silicon nitride (SiN) reactions, the silicon nitride radical is bound to the hydrocarbon by the nitrogen atom, and is the most stable product isomer despite the formal charges on nitrogen of −1 and silicon of +1. The Si–N triple bond is 1.581 Å and 1.571 Å long for the energetically favorable molecules silaisocyanoacetylene (HCCNSi) and silaisocyanoethylene (C_2H_3NSi), and 1.588 Å and 1.567 Å long for the energetically unfavorable molecules isosilaisocyanoacetylene (HCCSiN) and isosilaisocyanoethylene (C_2H_3SiN). In the reaction of silicon nitride (SiN) with acetylene, the bond length only elongates by 0.007 Å, while in the ethylene reaction it decreases by 0.004 Å. The unperturbed bond lengths in the silicon nitride (SiN) reactions are indicative of the large radius of the silicon atom of 1.10 Å and its associated large diffuse bonding orbitals. The Si–N bond is therefore not influenced by the presence of the rest of the molecule. The large radius of silicon being 0.40 Å larger than carbons of 0.70 Å results in very poor bonding overlap between the two as seen in the unfavorable isosilaisocyanoacetylene (HCCSiN) and isosilaisocyanoethylene (C_2H_3SiN) molecules. In comparison, the similar atomic radii of carbon and nitrogen differing by only 0.10 Å results in good bonding overlap in the energetically favorable molecules silaisocyanoacetylene (HCCNSi) and silaisocyanoethylene (C_2H_3NSi). The large radius of silicon makes the Si–C bonds 1.786 Å and 1.85 Å long, much longer than the N–C bond lengths of 1.296 Å and 1.365 Å. The unfavorable bonding overlap between silicon and carbon compared to nitrogen and carbon overcomes the beneficial electronic structure of isosilaisocyanoacetylene (HCCSiN) and isosilaisocyanoethylene (C_2H_3SiN) which have all atoms electronically balanced with no formal charge and a lone pair on the nitrogen – a common feature in nitrogen bearing molecules.

The reaction with ethynyl (CCH) and acetylene shows the diacetylene (HCCCCH) molecule to be more stable than the butatrienylidene ($CCCCH_2$) molecule by 183 kJ mol^{-1}. Diacetylene benefits from full bond conjugation between a triple bond of 1.207 Å followed by a single bond of 1.365 Å, no lone pairs of electrons and the molecule is highly symmetric owning a $D_{\infty h}$ point group. The butatrienylidene ($CCCCH_2$) has C_{2v} symmetry, owns a lone pair on the terminal carbon and has three carbon–carbon bonds of 1.282 Å for the terminal lone pair owning carbon, followed by 1.289 Å and 1.301 Å for the C–CH_2 bond, all corresponding to double bonds. It is clear that the difference in stability between diacetylene (HCCCCH) and butatrienylidene ($CCCCH_2$) is related to the lone pair on the terminal carbon in butatrienylidene ($CCCCH_2$) and to the difference in energetic stability between triple–single carbon–carbon bond conjugation and double–double carbon–carbon bonding. The ethylene reaction shows similar trends. Here, vinylacetylene is the most stable structure and has a triple–single–double bond conjugation system with bond lengths of 1.205 Å, 1.423 Å and 1.337 Å. The second most stable vinylacetylene ($CHCCHCH_2$) structure is butatriene (H_2CCCCH_2), which is only 32 kJ mol^{-1} higher in energy than vinylacetylene. Butatriene has three consecutive double carbon–carbon bonds with bond lengths 1.314 Å, 1.265 Å, and 1.314 Å. The importance of bond overlap in energetic stability of the two isomers is apparent since both isomers have their full complement of electrons involved in the bonding of the molecule with no lone pairs or static charges. The conjugated system of vinylacetylene is responsible for its greater stability due to the effective overlap of the π orbitals, while the bonding overlap between the double bonds is strong but less efficient. It should be noted that vinylacetylene also has a C_s point group compared with that of the symmetric D_{2h} point group of butatriene.

Interestingly, the silicon nitride and cyano radicals have their radical sites located on the opposite atoms. In the cyano radical, it is located on the carbon atom while in the silicon nitride case it is on the nitrogen. Since silicon and carbon are in

the same group and isovalent, one would expect a similar electronic configuration in this respect, however, the large radius and hence diffuse orbitals of silicon prevents it from being the best candidate for bonding to carbon or holding the radical center. In this respect, boron monoxide and cyano radicals show the greatest similarities, with both the electropositive atoms boron and carbon being bound to the hydrocarbon carbon molecules and their electronegative partner atoms nitrogen and oxygen at the end of the molecule giving enough 'space' for their lone pairs. Also, the nitrogen and oxygen atoms have only their triple and double bonds with their partners, while carbon and boron have their full complement of bonding electrons taken up. The silicon nitride reactions are therefore the odd ones out in these three cases, most notably due to the large radius and diffuse orbitals of the silicon atom. Silicon is located in the third period while carbon and boron are in the second period giving silicon an extra full shell of electrons. The differing location of the radical center and hence the resulting differing reactivity is seen here to be influenced by period rather than electronic structure and isovalency. This provides compelling motivation to further investigate the differing reactivity of isovalent radicals that span more than one period to find out the factors influencing the product isomers formed. Finally, the ethynyl reactions with the hydrocarbon reactant show a preference for the stronger triple bond of C–C and the use of the full complement of bonding electrons. This results in the diacetylene (HCCCCH) and vinylacetylene (C_2H_3CCH) molecules having no lone pairs and no formal charges, the most energy efficient configuration possible.

6. Summary

The reactions of isovalent $X^2\Sigma^+$ radicals – cyano (CN), boron monoxide (BO), silicon nitride (SiN), and ethynyl (C_2H) with unsaturated hydrocarbons acetylene and ethylene have been investigated using crossed molecular beams experiments and electronic structure calculations. The reactions were conducted at collision energies, $E_{collision}$ = 21–38 kJ mol^{-1}, and were found to proceed through emission of atomic hydrogen in overall exoergic reactions to form the most thermodynamically stable products: cyanoacetylene, boronylacetylene, silaisocyanoacetylene, and diacetylene [acetylene reactions] and vinyl cyanide, boronylethylene, silaisocyanoethylene, and vinylacetylene [ethylene reactions]. The reactions proceed most likely by addition of the radical by the radical bearing atom to the π electron orbitals as found by the electronic structure calculations. The addition pathways were found to be barrier-less and formed long lived collision complexes. In the acetylene reactions hydrogen emission occurs predominantly from the primary carbon of the initial intermediates i1 and i2, CHCHX while a small percentage can isomerize to i3 CH_2CX and subsequently emit a hydrogen from the secondary carbon. In the ethylene reactions hydrogen emission occurs with a slight predominance from i1 CH_2CH_2X (primary carbon), and the remainder from i2 CH_3CHX (secondary carbon). These distributions are reflected in the center-of-mass distributions which depict heavy peaking for the acetylene reactions and mild peaking in the ethylene reactions. The most striking difference in the group comes from silicon nitride, which forms silaisocyanoacetylene and silaisocyanoethylene products, bound by the nitrogen atom rather than the silicon atom in contrast to the cyano radical. These findings have been interpreted in respect to the location of the radical center on the diatomic, which is on nitrogen in silicon nitride and on carbon on the cyano radical. The location of the radical center and the product formed can be rationalized in terms of the Lewis structure which in turn is understood by the size of the atomic substituents and the resulting bonding overlap. Silicons large radius makes a triple bond with nitrogen impossible and hence it owns a lone pair forcing the radical center onto the nitrogen atom. In conclusion, the radicals display similar reactivity, reaction mechanisms and products formed across the group in respect to the radical location on the diatomic as expected from a isovalent group. The only difference applies to silicon nitride due to the location of the radical center on the diatomic.

The isovalent $X^2\Sigma^+$ radicals – cyano (CN), boron monoxide (BO), silicon nitride (SiN), and ethynyl (C_2H) – show distinct similarities, but also striking differences in their reactivity with unsaturated hydrocarbons acetylene and ethylene. These similarities and differences can be used to predict the behaviour of other unstudied di- and tri-atomic $X^2\Sigma^+$ radicals in reactions with unsaturated hydrocarbons. Further, understanding the role of a radicals Lewis structure and its atomic radii can aid in predicting the divergent behavior of isovalent reactions. Collecting experimental data on chemical reactivity in extreme environments such as astrochemistry and combustion environments under single collision conditions is non-trivial and therefore compiling accurate models is equally difficult. By

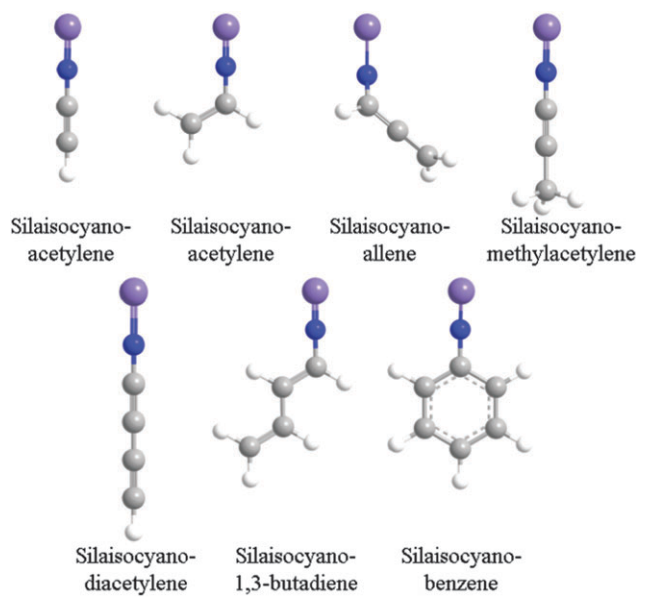

Fig. 7 Silaisocyano molecules formed in analogy to cyano addition – hydrogen atom elimination pathways and likely present in cold molecular clouds and in circumstellar envelopes of carbon rich stars such as IRC+10216.

providing the reaction dynamics of individual bimolecular reactions, and trends in reactivity of isovalent groups, theoretical models can more accurately predict chemical reactivity of bimolecular radical reactions in extreme environments. Note that among all isovalent radicals studied, reactions of silicon nitride (SiN) were the most difficult ones due to the relatively low concentration of the radical reactant. However, based on what we have learned from the reactions of silicon nitride (SiN) with acetylene and ethylene, we can predict that upon reaction of silicon nitride (SiN) with unsaturated hydrocarbons, the silicon nitride radical should bond with the nitrogen atom the unsaturated hydrocarbon. In analogy to cyano addition – hydrogen atom elimination pathways, we can predict the formation of hitherto unobserved silaisocyano molecules as compiled in Fig. 7. These molecules present excellent targets to be searched for with ALMA in cold molecular clouds and in circumstellar envelopes of carbon rich stars such as IRC+10216.

Acknowledgements

This work was supported by the US National Science Foundation (SiN; CHE-0948258) and by the Air Force Office of Scientific Research (BO; FA9550-12-1-0213).

References

1 I. Langmuir, *J. Am. Chem. Soc.*, 1919, **41**, 868–934.
2 I. Cherchneff, *Astron. Astrophys.*, 2012, **545**, A12/11–A12/14.
3 D. McElroy, C. Walsh, A. J. Markwick, M. A. Cordiner, K. Smith and T. J. Millar, *arXiv.org*, *e-Print Arch.*, *Astrophys.*, 2012, 1–18, arXiv:1212 6362v1211 [astro-ph SR].
4 D. L. Yang and M. C. Lin, *Adv. Ser. Phys. Chem.*, 1995, **6**, 164–213.
5 N. Balucani, *Int. J. Mol. Sci.*, 2009, **10**, 2304–2335.
6 H.-W. Wong, J. C. A. Nieto, M. T. Swihart and L. J. Broadbelt, *J. Phys. Chem. A*, 2004, **108**, 874–897.
7 K. B. Jefferts, A. A. Penzias and R. W. Wilson, *Astrophys. J.*, 1970, **161**, L87–L89.
8 M. Costes and C. Naulin, *Annu. Rep. Prog. Chem., Sect. C: Phys. Chem.*, 2013, **109**, 189–210.
9 P. Schilke, S. Leurini, K. M. Menten and J. Alcolea, *Astron. Astrophys.*, 2003, **412**, L15–L18.
10 K. D. Tucker, M. L. Kutner and P. Thaddeus, *Astrophys. J.*, 1974, **193**, L115–L119.
11 R. M. Roveri, M. E. Mendes and P. D. Singh, *Astron. Astrophys.*, 1988, **199**, 127–130.
12 A. McKellar, *Publ. Astron. Soc. Pac.*, 1940, **52**, 187–192.
13 C. Moureu and J. C. Bongrand, *Ann. Chim. Appl.*, 1920, **14**, 47–58.
14 F. F. Gardner and G. Winnewisser, *Astrophys. J.*, 1975, **195**, L127–L130.
15 L. C. L. Huang, O. Asvany, A. H. H. Chang, N. Balucani, S. H. Lin, Y. T. Lee, R. I. Kaiser and Y. Osamura, *J. Chem. Phys.*, 2000, **113**, 8656–8666.
16 L. Cartechini, G. Capozza, N. Balucani, A. Bergeat, P. Casavecchia and G. G. Volpi, *Eur. Space Agency, [Spec. Publ.], SP*, 2001, **496**, 309–312.
17 N. Balucani, O. Asvany, A. H. H. Chang, S. H. Lin, Y. T. Lee, R. I. Kaiser and Y. Osamura, *J. Chem. Phys.*, 2000, **113**, 8643–8655.
18 F. Leonori, R. Petrucci, X. Wang, P. Casavecchia and N. Balucani, *Chem. Phys. Lett.*, 2012, **553**, 1–5.
19 F. Leonori, K. M. Hickson, S. D. Le Picard, X. Wang, R. Petrucci, P. Foggi, N. Balucani and P. Casavecchia, *Mol. Phys.*, 2010, **108**, 1097–1113.
20 A. J. Trevitt, F. Goulay, G. Meloni, D. L. Osborn, C. A. Taatjes and S. R. Leone, *Int. J. Mass Spectrom.*, 2009, **280**, 113–118.
21 R. I. Kaiser and N. Balucani, *Acc. Chem. Res.*, 2001, **34**, 699–706.
22 R. I. Kaiser, *Eur. Space Agency, [Spec. Publ.], SP*, 2001, **496**, 145–153.
23 I. R. Sims, J.-L. Queffelec, D. Travers, B. R. Rowe, L. B. Herbert, J. Karthaeuser and I. W. M. Smith, *Chem. Phys. Lett.*, 1993, **211**, 461–468.
24 N. Balucani, O. Asvany, A. H. H. Chang, S. H. Lin, Y. T. Lee, R. I. Kaiser, H. F. Bettinger, P. v. R. Schleyer and H. F. Schaefer III, *J. Chem. Phys.*, 1999, **111**, 7472–7479.
25 N. Balucani, O. Asvany, A. H. H. Chang, S. H. Lin, Y. T. Lee, R. I. Kaiser, H. F. Bettinger, P. v. R. Schleyer and H. F. Schaefer III, *J. Chem. Phys.*, 1999, **111**, 7457–7471.
26 L. C. L. Huang, N. Balucani, Y. T. Lee, R. I. Kaiser and Y. Osamura, *J. Chem. Phys.*, 1999, **111**, 2857–2860.
27 A. Landera, A. M. Mebel and R. I. Kaiser, *Chem. Phys. Lett.*, 2008, **459**, 54–59.
28 R. I. Kaiser and A. M. Mebel, *Chem. Soc. Rev.*, 2012, **41**, 5490–5501.
29 A. M. Mebel, V. V. Kislov and R. I. Kaiser, *J. Am. Chem. Soc.*, 2008, **130**, 13618–13629.
30 B. Nizamov and S. R. Leone, *J. Phys. Chem. A*, 2004, **108**, 1746–1752.
31 D. Chastaing, P. L. James, I. R. Sims and I. W. M. Smith, *Faraday Discuss.*, 1998, **109**, 165–181.
32 A. B. Vakhtin, D. E. Heard, I. W. M. Smith and S. R. Leone, *Chem. Phys. Lett.*, 2001, **348**, 21–26.
33 F. Stahl, P. v. R. Schleyer, H. F. Schaefer III and R. I. Kaiser, *Planet. Space Sci.*, 2002, **50**, 685–692.
34 N. D. Marsh and M. J. Wornat, *Proc. Combust. Inst.*, 2000, **28**, 2585–2592.
35 B. Shukla and M. Koshi, *Anal. Chem.*, 2012, **84**, 5007–5016.
36 D. D. S. MacKay and S. B. Charnley, *Mon. Not. R. Astron. Soc.*, 1999, **302**, 793–800.
37 D. S. N. Parker, A. V. Wilson, R. I. Kaiser, T. Labrador and A. M. Mebel, *J. Am. Chem. Soc.*, 2012, **134**, 13896–13901.
38 D. S. N. Parker, A. V. Wilson and R. I. Kaiser, *J. Org. Chem.*, 2012, **77**, 8574–8580.
39 G. A. Oyedepo, C. Peterson and A. K. Wilson, *J. Chem. Phys.*, 2011, **135**, 094103.
40 D. S. N. Parker, F. Zhang, P. Maksyutenko, R. I. Kaiser and A. H. H. Chang, *Phys. Chem. Chem. Phys.*, 2011, **13**, 8560–8570.

41 D. S. N. Parker, F. Zhang, P. Maksyutenko, R. I. Kaiser, S. H. Chen and A. H. H. Chang, *Phys. Chem. Chem. Phys.*, 2012, **14**, 11099–11106.
42 B. Hussmann and M. Pfitzner, *Combust. Flame*, 2010, **157**, 822–833.
43 B. Hussmann and M. Pfitzner, *Combust. Flame*, 2010, **157**, 803–821.
44 A. I. Boldyrev, N. Gonzales and J. Simons, *J. Phys. Chem.*, 1994, **98**, 9931–9944.
45 E. P. J. L. a. W. G. Mallard, in *NIST Chemistry WebBook*, NIST Standard Reference Database Number 69.
46 G. Meloni, S. M. Sheehan, M. J. Ferguson and D. M. Neumark, *J. Phys. Chem. A*, 2004, **108**, 9750–9754.
47 R. I. Kaiser, P. Maksyutenko, C. Ennis, F. Zhang, X. Gu, S. P. Krishtal, A. M. Mebel, O. Kostko and M. Ahmed, *Faraday discuss.*, 2010, **147**, 429–478.
48 A. D. Becke, *J. Chem. Phys.*, 1993, **98**, 5648–5652.
49 C. Lee, W. Yang and R. G. Parr, *Phys. Rev. B: Condens. Matter Mater. Phys.*, 1988, **37**, 785–789.
50 G. D. Purvis III and R. J. Bartlett, *J. Chem. Phys.*, 1982, **76**, 1910–1918.
51 T. H. Dunning Jr., *J. Chem. Phys.*, 1989, **90**, 1007–1023.
52 M. J. Frisch, *et al.*, *Gaussian 98, revision A.11*, 2004.
53 H.-J. Werner, *et al.*, *MOLPRO, version 2006.1*, 2006.
54 K. A. Peterson and T. H. Dunning, *J. Phys. Chem. A*, 1995, **99**, 3898–3901.
55 R. I. Kaiser, F. Stahl, P. v. R. Schleyer and H. F. Schaefer III, *Phys. Chem. Chem. Phys.*, 2002, **4**, 2950–2958.
56 F. Zhang, S. Y. Kim, R. I. Kaiser, S. P. Krishtal and A. M. Mebel, *J. Phys. Chem. A*, 2009, **113**, 11167–11173.
57 R. D. Levine, *Molecular Reaction Dynamics*, 2005.
58 R. Grice and D. J. Smith, *Mol. Phys.*, 1993, **80**, 1533–1540.